

OFFICE OF NAVAL RESEARCH

Grant No: N00014-89-J-1412

R&T Code 413a005---03

Technical Report No. 23

Raman Spectroscopy Study of Solvation Structure in Acetonitrile/Water Mixtures

Prepared for publication in Analytical Chemistry

by

K. L. Rowlen and J. M. Harris

Departments of Chemistry
University of Utah
Salt Lake City, UT 84112

April 22, 1991



Classification	DTIS UNCLASSIFIED
Control	DTIC UNCLASSIFIED
Declassify	UNCLASSIFIED
Justification	UNCLASSIFIED
By	UNCLASSIFIED
Distribution	UNCLASSIFIED
Availability	UNCLASSIFIED
Storage	UNCLASSIFIED
Other	UNCLASSIFIED

A-1

Reproduction in whole, or in part, is permitted for
any purpose of the United States Government

* This document has been approved for public release and sale;
its distribution is unlimited.

01 4 30 013

TTL03

SEN03 Raman Spectroscopic Study of Solvation Structure in Acetonitrile/Water Mixtures

ADR03

AUT03 Kathy L. Rowlen¹ and Joel M. Harris^{*}

AAS03 Department of Chemistry, University of Utah, Salt Lake City, Utah 84112

ABS03

SEN03 Raman spectroscopy is used to probe the CN stretching frequency of acetonitrile as a function of concentration in water. SEN06 The CN band is modeled as the sum of two Gaussians. The SEN09 concentration dependence of area and width for each of the SEN12 Gaussian components provides experimental support of an equilibrium between two forms of acetonitrile in solution. In SEN15 addition the concentration dependence of each of the bands correlates well with the thermodynamically related Kirkwood-Buff Integrals (G_1). Specifically, both the vibrational SEN18 band width and G_1 exhibit maxima near $X_{\text{CH}_3\text{CN}} \approx 0.3$, suggestive of strong interaction between acetonitrile molecules. SEN21 The frequency shift of the CN band exhibits a linear dependence on the dielectric constant of protic solvents.

TXT03

SEN03

PAR03

SEN03 There has been considerable effort to define and understand the fundamental molecular interactions important in liquid chromatography (1-3). Although the solvophobic theory (1) is commonly invoked to explain retention in reversed-phase liquid chromatography (RPLC), recent studies have pointed out shortcomings in this model (3, 4). Using statistical thermodynamics, Dill (4) has demonstrated that retention in RPLC is driven by two classes of interactions: (1) the differences in chemical interactions of the solute in each of the phases, which affect the enthalpy of the system, and (2) changes in the entropy of the system. Studies of the importance of chemical interactions with the solvent have employed such techniques as solute solvatochromism (5, 6). SEN06 Solvent-stationary phase interactions have also received attention (7, 8). It is clear that the solvent plays a crucial role in establishing the "structure" of the stationary phase, which, SEN12 in turn, impacts the nature of solute retention. Recently several studies of solvent-stationary phase behavior have employed environment-sensitive probe molecules, such as SEN15 pyrene, adsorbed or immobilized at the surface (9). Spectroscopic changes in the probe provide information about the solute but only an indirect measure of surface characteristics. SEN18 An important experiment for understanding solute-induced changes in either the solvent-phase structure or the stationary-phase structure would involve monitoring some characteristic of the solvent and/or stationary phase directly. The SEN21 motivation for understanding solvent structure is found in the work recently conducted by Wirth (10, 11), in which the importance of shape selectivity in retention (related to structural order) was demonstrated spectroscopically.

PAR06

SEN03 Acetonitrile (CH_3CN) is one of the most widely used organic modifiers in reversed-phase liquid chromatography; it also has significant application in nonaqueous electrochemistry (12). SEN06 The Raman spectrum of CH_3CN has unique features in regions of low spectral interference; therefore, Raman spectroscopy of CH_3CN is an excellent choice for a direct probe of solvent microenvironment.

PAR09

SEN03 The CN stretch in acetonitrile exhibits a rather unique shift SEN06 to higher frequency when hydrogen bonded (13) or coordinated with Lewis acids (14). On the basis of the analogous SEN09 situation encountered with carbonyls, in which the CO stretch shifts to lower frequency when hydrogen bonded (15), one expects that coordination of the nitrogen lone pair electrons SEN12 would lengthen and thus weaken the CN bond. In the case of carbonyls, ^{13}C nuclear magnetic resonance (NMR) studies SEN15 show an apparent reduction in electron density (a shift to lower fields) about the carbonyl carbon and presumably an accompanying increase in electron density about oxygen, as SEN18 the concentration of a hydrogen bond donor is increased (16). SEN21 Similarly, NMR studies of CH_3CN -water mixtures show that

AC
7618

TXT03

PAR09

10 the ^{14}N resonance shifts to higher fields, an apparent increase
SEN15 20 in electron density about the nitrogen (17). Sadlej and Kecki
5 21 (18) employed a modified CNDO method to study the elec-
14 22 tronic structure of acetonitrile and its complexes with metal
SEN18 23 cations. They attributed the increased force constant of the
10 24 CN bond to a rehybridization, in which the 2p σ character of
SEN21 22 the lone pair is increased. Consideration of the partial an-
6 23 tubonding character of nitrogen's 2p σ orbital led to the con-
16 24 clusion that the removal of the lone pair electrons enhances
SEN24 25 the CN bond order. The authors observed that the corre-
7 26 sponding restructuring of π electrons would account for the
16 27 increased electron density about N (as measured by NMR).
SEN27 1 An increase in the force constant of the CN bond readily
13 28 accounts for the observed shift to higher frequencies when
CH₃CN is hydrogen bonded (13, 19).

PAR12

SEN03 1 The liquid structure of CH₃CN is also of interest and re-
SEN06 2 mains unresolved. Strong molecular interactions must account
3 for the high boiling point of CH₃CN (52 °C) as well as the fact
21 4 that ν_{CN} is 13 cm⁻¹ higher in the gas phase than in liquid (20).
SEN09 1 For comparison, the boiling point of methanol (similar density
11 2 and molecular weight), which exists as a hydrogen-bonded
SEN12 19 network in solution, is only 64.7 °C. It has been proposed that
7 20 a liquid-phase antiparallel alignment of two CH₃CN molecules
15 21 would result in a reduced dipole moment, therefore a weaker
SEN15 22 CN bond (21). This concept is supported by the observation
9 23 that a single CH₃CN molecule in the gas phase has a dipole
21 24 moment of 3.92 D, whereas the gaseous dimer has a dipole
SEN18 32 moment of 2.67 D (14). There is a large body of work that
10 33 suggests that CH₃CN is partitioned between monomers and
SEN21 34 dimers in solution (14, 20, 22). Griffiths (23) indicated that
6 35 it is unreasonable to expect a true CH₃CN dimer to exist in
18 36 solution and that free or unassociated CH₃CN is likely to be
19 37 in equilibrium with some undefined self-associated form of
SEN24 38 CH₃CN. Temperature-dependent studies of CH₃CN in a
4 39 variety of solvents appear to indicate that monomeric or free
18 40 CH₃CN does not exist in solution; rather, CH₃CN is organized
SEN27 41 as aggregates or loosely defined clusters (24). Several re-
28 42 searchers have reported that the CN stretching band of
12 43 CH₃CN in the liquid phase is composed of two overlapped
12 44 Gaussians: a narrow band, attributed to the monomeric or
SEN30 45 tree form of CH₃CN, and a broad band, attributed to some
4 46 organized form of CH₃CN (13, 23, 24). Infrared matrix iso-
15 47 lation studies of CH₃CN show two resolved bands in the CN
48 stretching region (14).

PAR15

SEN03 1 In order to employ CH₃CN and Raman spectroscopy as a
12 2 direct probe of solute/solvent or solvent/stationary phase
19 3 interactions, it is first necessary to understand the nature of
29 4 vibrational perturbations arising from solvent/solvent in-
SEN06 34 teractions. Here we report a detailed Raman spectroscopic
SEN09 35 study of CH₃CN in water. Presented in this work is the
4 36 behavior of the CN stretching vibration over the entire con-
17 37 centration range of acetonitrile/water mixtures and an ex-
24 38 ploration of the relationships between observed frequency
SEN12 39 shifts and solvent properties. Two groups have recently in-
6 40 vestigated the vibrational spectroscopy of CH₃CN/water
12 41 mixtures (13, 19), focusing primarily on the structural com-
20 42 position of water; neither group modeled the vibrational band
SEN15 43 structure. This work mathematically models the CN
4 44 stretching band (ν_{CN}) as the sum of two Gaussians, whose
18 45 behavior as a function of concentration supports the concept
27 46 of an equilibrium between at least two distinct CH₃CN species
SEN18 47 in solution. Further support for such an equilibrium is found
10 48 in the strong correlation between the CN frequency shift and
20 49 the dielectric constant of a variety of hydrogen-bond donor
29 50 solvents.

TXT06

EXPERIMENTAL SECTION

PAR18

SEN03 1 All solvents were spectrochemical or UV grade and were stored
12 2 over molecular sieves (1 Å \times 1 g/in.). Doubly distilled, HPLC
3 3 grade (1) Omnisolve) water was used in all experiments involving
24 4 water.

PAR21

SEN03 1 The 514.5-nm line from an argon ion laser (Lexel Model 95)
12 2 was employed as the excitation source. Plasma lines from the
3 3 source were eliminated with a combination of two PELLIN BROCHA

TXT06
PAR21

prisms (Optics for Research, ABDU-20) and a variable aperture. The 30-mW beam was focused to approximately 80 μm at the sample cell, a 0.1- \times 1-cm glass capillary (Kimax). Sample introduction was achieved via a 5-mL syringe connected to the capillary with 0.8-mm-i.d. Teflon tubing. All measurements were conducted at ambient temperature. Light from the cell was collected and collimated at 90° from excitation by a f/2 camera lens (Canon, f/50 mm) and then focused at the entrance slit of the spectrograph (0.5 m, Spex 1870) with a f/3.9 planoconvex lens. The entrance slit width was 60 (or 80) μm in all cases, corresponding to a spectral bandwidth of 3.6 cm^{-1} . A colloidal glass (RG-530, Schott) high-pass filter, placed in front of the entrance slit, served to remove scattered source light. A 600 groove/mm grating dispersed the light across a Thomson THF7882CDA charge-coupled device (CCD, Photometrics). With the long axis (576 channels) oriented in the direction of wavelength dispersion, a spectral region of approximately 600 cm^{-1} was sampled simultaneously at approximately 1 cm^{-1} /channel. The CCD controller was linked to a Mac IIcx via a general purpose interface board (GPIB, National Instruments). The interface software, OMA, was written by Marshall Long (Yale, Applied Physics Department).

PAR24

For all spectra presented in this work, a preflash was used and the charge from 383 columns was binned along the slit axis for signal-to-noise improvement. It has recently been reported that binning in this direction can result in artificial band broadening (23). However, we are confident that the asymmetry found in the bands reported herein is physicochemical in nature based on the fact that similar band shapes have been observed and reported by workers using monochromator/PMT systems (13, 23, 24) and the following study of charge trapping conducted in this lab. The effect of charge trapping on peak parameters was quantified by using a single Lorentzian fit to the 214- cm^{-1} band of CCl_4 . We found charge trapping to be of concern only at low signal intensities, <70,000 photoelectrons, in which no "preflash" had been used to uniformly irradiate the CCD. With the preflash, no band distortions were observed.

PAR27

The CH , CN , and CC stretching frequencies (2942, 2249, 918 cm^{-1}) (26) in dry CH_3CN were used as reference points for band position measurements in other solvents. These reference points were established prior to each set of measurements in a given region. To avoid mechanical backlash errors, the spectrograph settings were not varied during any group of measurements in a particular region. All quantitative measurements were made, minimally, in triplicate. Concentrations (M) were calculated taking into account the nonideal volume of mixing for CH_3CN and water, as tabulated by Katz et al. (27). Measured band areas were corrected for refractive index effects as indicated by Bauer et al. (28). The correction values vary less than 2% over the investigated concentration range.

PAR30

Data processing was conducted on an IBM AT compatible computer. Conversion of binary files from the Macintosh disk operating system to MS-DOS was carried out with the Apple File Exchange program. Peak modeling to Gaussian functions was achieved with the program Curvefit (χ^2 minimization) in SpectraCalc (Galactic Industries, V2.1). The spectra could not be modeled as Lorentzian functions.

TXT09

RESULTS AND DISCUSSION

PAR33

Acetonitrile in Water. CN Stretch. Figure 1 shows the CN stretching band (ν_{CN}) in neat acetonitrile. The frequency maximum shifts linearly to higher frequencies as the molar concentration of CH_3CN in water decreases, from 2249 cm^{-1} in neat CH_3CN to 2256 cm^{-1} at 1.9 M (a change of 7 ± 0.4 cm^{-1} , from eight measurements). In order to investigate the possibility and behavior of overlapped bands as a function of concentration, both ν_{CN} and ν_1 , as labeled in Figure 1, were modeled by using the Curvefit program in Spectra Calc. ν_1 is a combination band arising from the symmetric bend of CH_3 and the CC stretch (29). Although ν_1 is not part of the CN stretch, it was included in the model in order to improve the accuracy of the fit. The best fit to the CN band shape is two overlapped Gaussians (ν_{II} and ν_{III}).

PAR36

Band Area. As is observed from Figure 2, the total measured area ($\nu_{\text{II}} + \nu_{\text{III}}$) is linear with concentration. Figure 3 shows the behavior of ν_{II} and ν_{III} as a function of concentration. Assuming that both ν_{II} and ν_{III} are due only to the stretching mode of CN (30), the fact that there are two bands, each

FIG 1 (009, 3-4)

FIG 2 (006, 7-8)
FIG 3 (009, 3-4)

TXT09
 PAR36

26 having a unique concentration dependence, implies that
 27 acetonitrile exists in at least two distinct forms in solution.
 SEN15 28 Since both ν_{11} and ν_{33} are present in pure (dry) CH₃CN, neither
 29 of the two Gaussian components can be attributed to hydrogen
 SEN18 30 bonding with water. This may not be true for low concen-
 31 trations of CH₃CN in water. Both components have nearly
 32 equivalent areas from 2 to 8 M CH₃CN which, in agreement
 33 with previous observations (20, 24), suggests that strong inter-
 34 actions between CH₃CN molecules must prevail even at
 SEN24 35 low concentrations. Between 5 and 12 M, the area of ν_{11}
 36 increases at a rate faster than that of ν_{33} . Near 12 M ($X_{\text{CH}_3\text{CN}}$
 37 ~ 0.3–0.35) CH₃CN, there appears to be a transition between
 SEN30 38 ν_{11} and ν_{33} . At concentrations greater than 15 M ($X_{\text{CH}_3\text{CN}} \sim$
 39 0.55), ν_{33} becomes the dominant band. The relationship be-
 40 tween areas at concentrations greater than 12 M is consistent
 41 with a picture of the liquid in which self-associated CH₃CN,
 42 represented by ν_{33} , is favored at high concentrations.

PAR39

SEN03 1 Attempts to quantify a particular species, such as CH₃CN
 2 monomer or dimer, using the measured band areas were un-
 SEN06 3 successful. Substitution of activity (31) for molarity did no
 SEN09 4 improve the situation. However, as Pimentel and McClellan
 5 (32) have pointed out, one would only expect a clear, definable
 6 equilibrium between, for example, monomer and dimer in
 7 solution if the dimer were cyclic with no additional sites
 SEN12 8 available for interaction. Consideration of the data presented
 9 here and evidence that the methyl group is strongly involved
 10 in determining the structure of liquid CH₃CN (33) lead to the
 11 conclusion that no simple equilibrium between definite
 12 CH₃CN species exists in solution.

PAR42

SEN03 1 *Bandwidth.* Figure 4 shows the bandwidth (full width at
 2 half maximum) as a function of mole fraction CH₃CN; mole
 3 fraction is used in this case, rather than molarity, to facilitate
 4 comparison with thermodynamic parameters. Note, however,
 5 that the maximum in bandwidth occurs at the same concen-
 6 tration as the transition observed for band areas (~12 M).

PAR45

SEN03 1 Matteoli and Luciano (34) recently calculated the values
 2 of G_{ij} for CH₃CN/water mixtures from the Kirkwood-Buff
 3 integrals (35)

$$G_{ij} = (g_{ii} - 1)4\pi r^2 dr \quad (1)$$

20 where g_{ii} is the radial distribution function and r is the average
 21 distance between adjacent molecules. G_{ij} is a measure of the
 22 tendency for dissimilar molecules to interact and G_{ii} is a
 23 measure of interaction tendency between like molecules. G_{ij}
 24 and G_{ii} are related to thermodynamic properties as described
 25 by the following equations

$$G_{ij} = RTK_T - V_i/\bar{V}_jDV \quad (2)$$

$$G_{ii} = G_{ij} + \bar{V}_j/(D - V_i)x_i \quad (3)$$

$$D = 1 + x_i(\partial \ln \alpha_i / \partial x_i)_{TP} \quad (4)$$

26 where R , T , K_T , V_i , α_i , x_i , and V represent the gas constant,
 27 temperature, isothermal compressibility coefficient of the
 28 solution, partial molar volume, activity coefficient, mole
 29 fraction, and the volume per mole of mixture, respectively.
 SEN12 30 Matteoli and Luciano found, for both CH₃CN and water, that
 SEN15 31 G_{ij} exhibited a maximum near $X_{\text{CH}_3\text{CN}} = 0.3$ ($= X_{\text{max}}$). Such
 32 a maximum implies a strong tendency for like molecules to
 33 associate (G_{ii} vs X_i decreases monotonically for an ideal
 34 mixture). On the basis of the overall shape of the G_{ij} vs X_i
 35 curve, the authors divided the solution behavior into three
 36 categories, the maximum serving as the transition between
 37 solvation and self-association. At $X_{\text{CH}_3\text{CN}} < X_{\text{max}}$, the trend
 38 of G_{ij} for water indicated that small amounts of CH₃CN could
 39 significantly affect the structure of water. The structure of
 40 CH₃CN remains primarily unaffected by small amounts of
 41 water. At $X_{\text{CH}_3\text{CN}} > X_{\text{max}}$, the authors noted that the smooth
 42 trend of G_{ij} toward neat CH₃CN was suggestive of direct
 43 interaction between CH₃CN molecules.

PAR48

SEN03 1 The bandwidths of both ν_{11} and ν_{33} exhibit a maximum near
 2 $X_{\text{CH}_3\text{CN}} = 0.3$. The maximum is more pronounced for ν_{11}
 3 (self-associated CH₃CN); thus, the behavior of the bandwidth

FIG. 4 (006, 3-4)



REQU 1 (003,19-20)

REQU 2 (009,15-16)

REQU 3 (009,15-16)

REQU 4 (009,15-16)

TXT09
PAR48

SEN09 1 may be more closely associated with CH₃CN. CH₃CN inter-
actions rather than CH₃CN/H₂O interactions. Since both the
2 bandwidths and band areas undergo dramatic transitions at
3 the concentrations of similar activity for the Kirkwood
4 integrals, there appears to be a relationship between the solvent
5 structure probed by Raman spectroscopy and the thermo-
SEN12 6 dynamic properties of the solution. In addition, it is inter-
7 esting to note that the bandwidth maximum occurs at pre-
8 cisely the point at which the partial molar excess volumes of
SEN15 9 CH₃CN and water are equal (26). Kamazawa and Kitagawa
10 (33), using Raman difference spectroscopy to analyze the
11 symmetric CH stretch of CH₃CN in water, found that a plot
12 of homogeneous frequency shift (the shift attributed to
13 self-associated molecules) vs mole fraction was very similar
SEN18 14 to the plot of partial molar volume vs mole fraction. The
15 authors interpreted this as an indication that the frequency
16 shift was related to the structure of the solution.

PAR51

SEN03 1 *Frequency Shifts.* Figure 5 shows the center frequency of
SEN09 2 ν_{CH_3} and ν_{H} vs mole fraction. The measured center frequency
3 for ν_{CH_3} is dominated by ν_{CH_3} and therefore exhibits similar
SEN12 4 behavior. For the purpose of discussion, we will assume that
5 an CH₃CN dimer is representative of self-associated CH₃CN.
SEN15 6 Thomas and Thomas-Orville proposed the structure of an
7 CH₃CN dimer as

RID AC5B11a (015.12-13)

Author
File MSS
Page 10

FIG 5 (006, 3-4)

SEN18

1 This structure also derives from both neutron diffraction
2 studies and ab initio calculations as the most energetically
3 stable CH₃CN dimer orientation for intermolecular distances
SEN21 4 less than 5 Å (22). According to Pauling (37), due to the large
5 dipole moment, the CN bond can possess as much as 21% ionic
SEN24 6 character. Bulk solvent effects, such as dielectric properties,
7 are therefore expected to play a key role in determining the
SEN27 8 strength of intermolecular interactions. If self-association
9 results in a lower CN force constant, through partial can-
10 cellation of dipole moments—as mentioned in the
11 Introduction—then the effective solvation of self-associated
SEN28 12 CH₃CN should result in an increase in ν_{CH_3} . Hydrogen bonding,
13 in which the partially antibonding lone pair electrons are
14 removed from the CN bond, should also result in an increase
SEN33 15 in ν_{CH_3} . Therefore, in the case of protic solvents, the magnitude
16 of shift in ν_{CH_3} is expected to have a complicated dependence
17 on both solvent dielectric properties and hydrogen-bond
SEN36 18 strength. It is worth noting that the center frequency of ν_{H}
19 exhibits a linear dependence on molarity, whereas ν_{CH_3} has a
SEN39 20 more complicated dependence. The dielectric constant of
21 CH₃CN/water mixtures varies approximately linearly with
SEN42 22 molarity (38). In addition to dielectric and hydrogen-bond
23 effects, there is evidence that suggests that hydrophobic
24 interactions may also play a role in CH₃CN aggregation at high
25 water concentrations (33, 34).

PAR54

SEN03 1 To test the importance of dielectric effects, a study of
2 CH₃CN ($X_{\text{CH}_3\text{CN}} = 0.037$, 1.9 M) in a variety of protic (hydro-
SEN06 3 gen-bond donating) solvents was conducted. Figure 6
4 shows the frequency shift from 2249 cm⁻¹ (ν_{CH_3} in pure CH₃CN)
5 as a function of dielectric constant. The frequency shift for
6 CH₃CN would, of course, be zero but is not shown on the graph
SEN12 7 because it is not a hydrogen-bond donor. Note that water ($\epsilon = 78.5$) is the only solvent in the figure that has a higher
8 dielectric constant than CH₃CN ($\epsilon = 38.8$). The difference
SEN15 9 in the magnitude of shift for water and its nearest neighbor
10 (MeOH) is significant. The linearity of the plot as well as the
11 magnitude of the shift for water indicates a strong dependence
SEN18 12 on the dielectric properties of the solvent. Plots of frequency
13 shift vs (1) dipole moment, (2) refractive index, (3) polariza-
14 bility (calculated from the Clausius-Mossotti equation), and
15 (4) orientation polarizability (Δr) (calculated from the Linnert
16 equation (39)) were all nonlinear or uncorrelated. For the
17 above calculations, it was assumed that the bulk properties
SEN21 18 of the mixture were equivalent to those of the solvent. This
19 assumption is valid for dilute solutions, as is true for $X_{\text{CH}_3\text{CN}}$
SEN24 20 = 0.037. Although bulk dielectric properties appear to play
21 a primary role in determining ν_{CH_3} , hydrogen bonding must
22 also take place. Recent ab initio calculations have estimated
SEN33 23

FIG 6 (006, 3-4)

Author
File MSS
Page 11

TXT09

PAR54

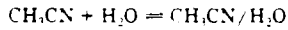
8 the hydrogen-bond strength of CH₃CN/water to be approximately 4 kcal/mol (41). The OH stretch of water is quite sensitive to dilution with CH₃CN, shifting more than 100 cm⁻¹ over the concentration range studied. The magnitude of the shift is characteristic of hydrogen-bond donors (42).

PAR57

SEN03 1 Both the CC and CH stretching modes shift to higher frequency upon dilution of CH₃CN in water. The slopes of SEN06 12 center frequency vs molarity are 0.39 and 0.27 for ν_{CC} and ν_{CH}, respectively.

PAR60

SEN03 1 *Associated Species.* Katz et al. (27) recently suggested that SEN06 9 mixtures of MeOH/water, CH₃CN/water, and tetrahydrofuran (THF)/water should be regarded as ternary solvent systems, the three components being free solvent (i.e., not 14 associated with water), free water, and a solvent/water complex. 19 The authors postulated that deviation from ideal mixing, 22 as well as chromatographic anomalies, could be explained in 26 terms of the presence of this third (solvent/water) species. 31 SEN12 1 They mathematically modeled the volume of the mixing curve 34 by assuming that the molar volume of all three components 37 remained constant over the entire range of compositions. 40 SEN15 1 However, it is well documented that the molar volume of 43 components in nonideal solutions does indeed vary (42). In 46 addition, in describing CH₃CN/water mixtures as a simple 51 equilibrium



$$K_{eq} = [\text{CH}_3\text{CN}/\text{H}_2\text{O}] / [\text{CH}_3\text{CN}][\text{H}_2\text{O}] \quad (5)$$

12 the activities of water, CH₃CN, and CH₃CN/H₂O must be 21 used to calculate K_{eq}. Based on the activities reported by 24 French (31), the equilibrium in eq 5 would result in an 27 CH₃CN/H₂O complex whose activity remains constant from 30 0.2 to 0.7 mole fraction CH₃CN. The model used by Katz et 33 al. results in a continuously varying associated complex (as 36 measured by volume fraction) that exhibits a maximum near 39 X_{CH₃CN} ≈ 0.25. Based on the results of Matteoli and Luciano 42 (34), the minimum in the volume of mixing may be due to 45 effective "packing" of CH₃CN within the water structure 48 rather than a maximum in CH₃CN/H₂O complexes. While 51 it is intuitively satisfying to consider associated species in 54 binary mixtures, the model Katz et al. have chosen may not 57 be an accurate description.

PAR63

SEN03 1 Taking into account both solvent/solvent and solvent/solute 3 species, CH₃CN/water mixtures are more thoroughly 6 described as having at least six general components: CH₃CN, 9 CH₃CN/(CH₃CN/H₂O), CH₃CN/H₂O, H₂O, and (H₂O)_n. As 12 the concentration is varied, the distribution of interactions 15 must also vary. At low CH₃CN concentrations (X_{CH₃CN} < 0.3), 18 due to the strength of attractive forces between CH₃CN molecules, it is not unreasonable that both free (e.g., CH₃CN, 21 CH₃CN/H₂O) and self-associated (e.g., CH₃CN/CH₃CN) 24 SEN12 33 CH₃CN exist. The stable association of CH₃CN molecules 27 would eventually serve to disrupt the water structure. Based 30 on the observations of Singh and Krueger (19), in which the 33 3225-cm⁻¹ band in water vanishes as CH₃CN is increased to 36 X_{CH₃CN} = 0.47, the structure of water appears to be dominant 39 up to X_{CH₃CN} ≈ 0.3. Beyond that point, both the structure 42 of water and of CH₃CN approach their least structural form. 45 SEN18 1 The maximum excess entropy of mixing (X_{CH₃CN} ≈ 0.55), 48 rather than the volume of mixing, is likely to be correlated 51 with the largest degree of association between CH₃CN and 54 water (see Figure 7 (31, 43)). At CH₃CN mole fractions greater 57 than 0.55, the structure of CH₃CN dominants. This concept 60 is supported by the fact that the area of band III, attributed 63 to self-associated CH₃CN, becomes the dominant factor at 66 CH₃CN mole fractions greater than 0.55.

PAR66

SEN03 1 Although there are undoubtedly a variety of effects that 3 influence the degree of association between CH₃CN molecules. 6 It is possible that the dominant driving force for aggregation 9 progresses from hydrophobic to electrostatic as the CH₃CN 12 concentration is increased. At high water concentrations, the 15 dielectric constant of the solution is high; therefore, electrostatic 18 interactions are minimized while the tendency for hy-

REQU 5a 018.11-12

SEQU 5 018.11-12

FIG 7 (021.34-35)

TXT09

PAR66

SEN09 23 hydrophobic interactions is maximized. As mentioned above,
3 the shape of the G_1 vs X_{CH_3CN} curve suggests that for X_{CH_3CN}
17 > 0.3 direct interactions between CH_3CN molecules occurs.
SEN12 1 If one defines direct interaction as that which occurs at in-
12 termolecular separation distances $\leq 5 \text{ \AA}$, the antiparallel
20 orientation of two CH_3CN molecules is the most stable dimer
SEN15 30 (27). A dimer, in which the opposite partial charges are
11 aligned, seems reasonable at high CH_3CN concentrations.
SEN18 1 High CH_3CN concentrations would facilitate stronger elec-
3 trostatic attraction via decreased average intermolecular
14 distances and a lower dielectric constant.

PAR69

SEN03 1 *Chromatographic Implications.* The presence of a variety
SEN06 7 of CH_3CN species in solution would result in complicated
SEN09 16 equilibria for solvation of other solutes. Shifts in the equilibria,
8 which occur as the solvent composition is varied, may account
SEN12 16 for anomalies in chromatographic retention (44). McCormick
3 and Karger (45) have reported the adsorption isotherms for
12 MeOH, CH_3CN , and THF on a hydrophobic stationary phase
SEN15 21 (C-18). Both CH_3CN and THF exhibited dramatic maxima
3 near 50% ($X_{CH_3CN} = 0.25$) and 70% (v/v) organic modifier,
SEN18 13 respectively. For acetonitrile/water mixtures, more than twice
4 as much CH_3CN is adsorbed to the surface at mobile-phase
SEN21 18 composition $X_{CH_3CN} = 0.25$ than at $X_{CH_3CN} = 0.55$. In ac-
11 cordance with the soiophobic theory, the authors attributed
14 the decreased adsorption of the organic modifier to reduced
19 interfacial concentration in the mobile phase, *i.e.*, being the
22 driving force for removal of organic modifier from solution.
SEN24 1 However, the removal of organic modifier from solution is
12 unlikely to be driven by entropy, since (1) the process of
15 concentrating solvent/solute at the interface is accompanied
19 by a decrease in entropy due to structuring of the alkyl phase
24 (3, 4) and (2) the solvation of CH_3CN in water is purely en-
27 tropy driven (see Figure 7). If hydrophobic expulsion were
5 exclusively responsible for concentrating CH_3CN at the sur-
9 face, the process should be most favorable when the enthalpy
13 of mixing is least favorable, and such is not the case. As shown
17 in Figure 7, the interaction between CH_3CN and water is most
21 endothermic (least favorable) at mole fractions much higher
25 ($X_{CH_3CN} = 0.65$) than the observed maximum in the isotherm.
SEN33 1 These conclusions are in agreement with studies that suggest
12 that hydrophobic expulsion is not the dominant interaction
15 in RPLC retention (3).

PAR72

SEN03 1 As mentioned previously, Katz et al. (27) suggest that
11 anomalies in solute retention can be explained in terms of
14 associated solvent species, each of which has unique inter-
17 actions with the stationary phase. As the mobile phase is
20 varied, the chemical characteristics of the stationary phase
23 are determined by the relative concentrations of the individual
26 species (e.g., CH_3CN , $CH_3CN \cdot H_2O$, H_2O). The spectroscopic
29 evidence presented here, in conjunction with thermodynamic
SEN06 11 considerations, supports this proposal. The activity of CH_3CN
15 in water increases drastically over the range $X_{CH_3CN} = 0-0.25$,
SEN15 18 at which point it levels off (31). Based on the area and
21 bandwidth behavior of v_H and v_{H_2O} , the region of increasing
24 activity may be due to changes in the ratio of hydrogen-bonded
SEN18 28 to self-associated species. The minimal changes in CH_3CN
1 activity at high CH_3CN concentrations may be due to the
SEN21 31 formation of a stable self-associated CH_3CN complex. The
1 maximum in the adsorption isotherm reported by McCormick
14 and Karger (45) corresponds to the transition point in activity
17 and quite closely with the transition in CH_3CN microenvi-
20 ronment as reported here.

TXT12

SEN03 1

PAR73

SEN03 1 **CONCLUSION**
10 Raman spectroscopy has been used to quantify vibrational
10 frequency changes in acetonitrile under hydrogen-bond con-
16 ditions. The CN band of acetonitrile was shown to consist
11 of overlapped Gaussians (II and III). The behavior of bands
16 II and III as a function of concentration in water provides
17 experimental support for an equilibrium between CH_3CN
18 species in solution. Comparison of band behavior with the
19 Kirkwood-Buff G values demonstrates a relationship between
20 solute microenvironment and the thermodynamic properties
23 of the solution. The center frequency of the individual bands

TXT12
PAR75

as a function of concentration in water was discussed in terms of both dielectric and hydrogen-bond effects.

TXT15

PAR78

SEN00

ACKNOWLEDGMENT

SEN03 We thank W. R. Fawcett for helpful discussions on the electronic structure of CH₃CN and for directing us to valuable references.

FNN02

RFH00

SYF03

SEN00

Present Address: Department of Chemistry, University of Colorado, Boulder, CO 80309

SYF06

SEN00

*Address correspondence to this author

FNP03

SEN03

1) Horvath, C. Melander, W., Molnar, I. J. *Chromatogr.* 1978, 125, 129

FNN03

FNP06

SEN03

2) Michaels, J. J., Dorsey, J. G. *J. Chromatogr.* 1988, 457, 85

FNN04

FNP09

SEN03

3) Dorsey, J. G., Gill, K. A. *Chem. Rev.* 1988, 89, 331

FNN05

FNP12

SEN03

4) Gill, K. A. *J. Phys. Chem.* 1987, 91, 1980

FNN06

FNP15

SEN03

5) Sadek, P. J., Carr, P. W., Doherty, R. M., Kamlet, M. J., Taft, R. W., Abraham, M. H. *Anal. Chem.* 1985, 57, 2971

FNN07

FNP18

SEN03

6) Johnson, B. P., Khaleki, M. G., Dorsey, J. G. *J. Chromatogr.* 1987, 384, 221

FNN08

FNP21

SEN03

7) Lochmuller, C. H., Colborn, A. S., Hunnicut, M. L., Harms, J. M. *J. Am. Chem. Soc.* 1984, 106, 4077

FNN09

FNP24

SEN03

8) Lochmuller, C. H., Colborn, A. S., Hunnicut, M. L., Harms, J. M. *Anal. Chem.* 1983, 55, 1344

FNN10

FNP27

SEN03

9) Carr, P. W., Harms, J. M. *Anal. Chem.* 1988, 58, 626

FNN11

FNP30

SEN03

10) Wirth, M. J. *J. Phys. Chem.* 1987, 91, 3926

FNN12

FNP33

SEN03

11) Wirth, M. J., Hahn, D. A. *J. Phys. Chem.* 1987, 91, 3099

FNN13

FNP36

SEN03

12) Bard, A. J., Faulkner, L. R. *Electrochemical Methods*; Wiley: Canada, 1980

FNN14

FNP39

SEN03

13) Kabisch, V. *Z. Phys. Chem. (Leipzig)*, 1982, 263, 48

FNN15

FNP42

SEN03

14) Freedman, T. B., Nixon, E. P. *Spectrochim. Acta* 1972, 28A, 1375

FNN16

FNP45

SEN03

15) Nyquist, R. A. *Appl. Spectrosc.* 1980, 44, 426

FNN17

FNP48

SEN03

16) Nyquist, R. A., Putzig, C. L., Hasha, D. L. *Appl. Spectrosc.* 1988, 43, 1049

FNN18

FNP51

SEN03

17) Lowenstein, A., Margalit, Y. *J. Phys. Chem.* 1985, 89, 4152

FNN19

FNP54

SEN03

18) Sadlej, J., Kocik, Z. *Roczn. Chem.* 1989, 43, 2131

FNN20

FNP57

SEN03

19) Singh, S., Krueger, P. J. *J. Raman Spectrosc.* 1982, 13, 178

FNN21

FNP60

SEN03

20) Sadlej, J. *Spectrochim. Acta* 1979, 35A, 681

FNN22

FNP63

SEN03

21) Thomas, B. H., Thomas-Orville, W. J. *J. Mol. Struct.* 1989, 3, 191

FNN23

FNP66

SEN03

22) LaMenna, G. *Chem. Phys. Lett.* 1983, 103, 55

FNN24

FNP69

SEN03

23) Griffiths, J. E. *J. Chem. Phys.* 1973, 59, 751

FNN25

FNP72

SEN03

24) Lowenschuss, A., Yellin, N. *Spectrochim. Acta* 1975, 31A, 207

FNN26

FNP75

SEN03

25) Pemberton, J. E., Sobociński, R. L., Sims, G. R. *Applied Spectrosc.*

FNN27

FNP78

SEN03

1980, 44, 328

FNN28

FNP81

SEN03

26) Dolish, F. R., Fateley, W. G., Bentley, F. F. *Characteristic Raman Frequencies of Organic Compounds*; Wiley: New York, 1973

FNN29

FNP84

27) Katz, E. D., Ogan, K., Scott, R. P. *J. Chromatogr.* 1988, 352, 67

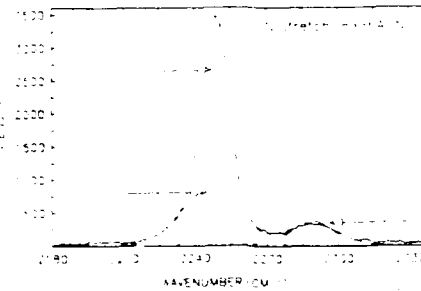
6/1984
Page 19

UNIT NO. 106
C61-AUCB11 AC00062K V-63 (top)

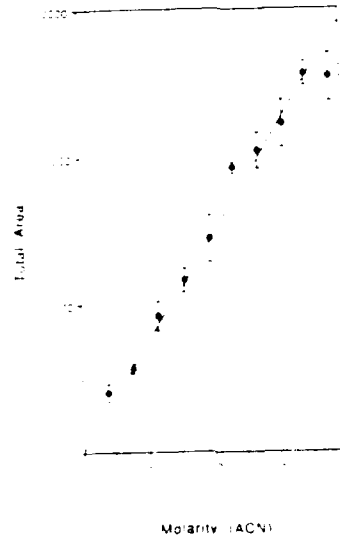
60610

- NN29**
FNP84
SEN03
FNN30
FNP87
SEN03
FNN31
FNP90
SEN03
FNN32
FNP93
SEN03
FNN33
FNP96
SEN03
FNN34
FNP99
SEN03
FNN35
FNP102
SEN03
FNN36
FNP105
SEN03
FNN37
FNP108
SEN03
FNN38
FNP111
SEN03
FNN39
FNP114
SEN03
FNN40
FNP117
SEN03
FNN41
FNP120
SEN03
FNN42
FNP123
SEN03
FNN43
FNP126
SEN03
FNN44
FNP129
SEN03
FNN45
FNP132
SEN03
FNN46
FNP133
SEN03
RCP03
SEN03
SEN09
- 28) Bauer, J.; Brauman, J. I.; Pecora, R. J. *J. Chem. Phys.* 1975, 63, 53
29) Addison, C. C.; Amos, D. W.; Sutton, D. *J. Chem. Soc. A* 1968, 2287
30) Wofford, B. A.; Bevan, J. W.; Olson, W. B.; Lafferty, W. *J. Chem. Phys.* 1985, 83, 5188
31) French, H. T. *J. Chem. Thermodyn.* 1987, 19, 1155
32) Pimentel, G. C.; McClellan, A. C. *The Hydrogen Bond*. Reinhold, New York, 1960
33) Kamada, K.; Kitagawa, T. *J. Phys. Chem.* 1986, 90, 1077
34) Mateo, E.; Luciano, L. *J. Chem. Phys.* 1984, 80, 2856
35) Kirkwood, J. G.; Bunn, F. P. *J. Chem. Phys.* 1951, 19, 114
36) Handa, Y.; P. Benson, G. C. *J. Solution Chem.* 1981, 10, 391
37) Pauling, L. *The Nature of the Chemical Bond*. Cornell University Press, Ithaca, NY, 1960
38) Ashford, L. J. *Dielectric Properties of Binary Solutions*. Pergamon Press, New York, 1981
39) Weast, R. C. Ed. *Handbook of Chemistry and Physics*, 62nd ed., CRC, Boca Raton, FL, 1981
40) Lakowicz, J. R. *Principles of Fluorescence Spectroscopy*. Plenum Press, New York, 1983
41) Damewood, J. R.; Kumpf, R. A. *J. Phys. Chem.* 1987, 91, 4444
42) Moreau, J.; Chauvet, G. *Thermochim. Acta* 1975, 13, 185
43) Christensen, J. J.; Rowley, R. C.; Carl, R. M. Eds. *Handbook of heats of Mixing*. Wiley, New York, 1988
44) Raymond, C.; Chung, G. N.; Mayer, J. M.; Testa, B. *J. Chromatogr.* 1987, 391, 97
45) McCormick, R. M.; Karger, B. L. *Anal. Chem.* 1980, 52, 2249
- RECEIVED for review September 24, 1990; Accepted February 15, 1991. This work was supported in part by the Office of Naval Research.

UNIT NO. 1007
Date: 10/18/91 AC: 000762K - 1.00 (00)



AP001
AP006 12
AP009 10
Figure 1 CN stretch (2249 cm^{-1}) in neat acetonitrile with a 10-s integration time. The dashed lines represent the modeled Gaussians. The data are unsmoothed.



AP001
AP006 12
Figure 2 Total area as a function of concentration. error bars are
AP006 12 ±3. The equation for the line is $y = 1458 (\pm 34)$.

UNIT NO. 4008
Gal. 11 AC5B11 AC900762K V-63 1010

910319

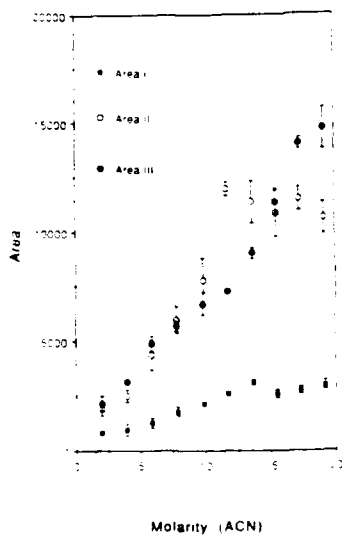


Figure 3. Area of individual Gaussian components as a function of CH₃CN molarity. In some cases, the symbol width exceeds the measured error.

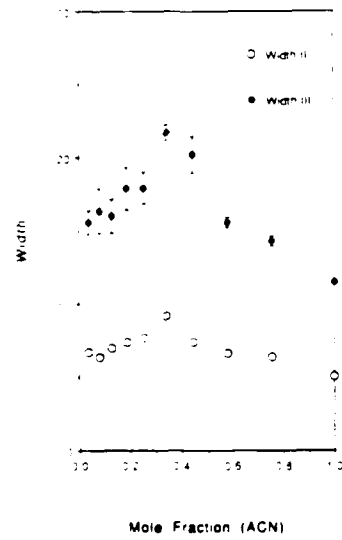


Figure 4. Bandwidth (full width at half-maximum) as a function of concentration. Error bars are $\pm \sigma$. For band II, the symbol width is larger than the measured error.

UNIT NO 1009
Gal. 12 AC5B11 AC000762K 1-63 1010

940319

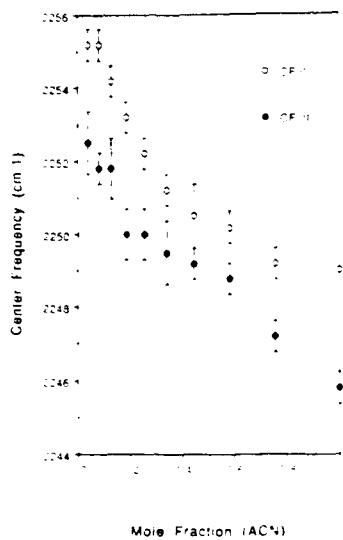


Figure 5. Center frequency as a function of concentration; error bars are $\pm \sigma$.

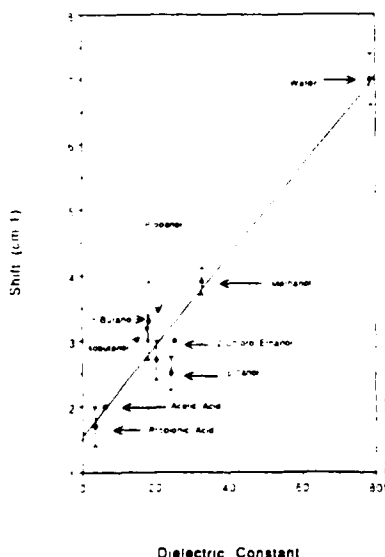
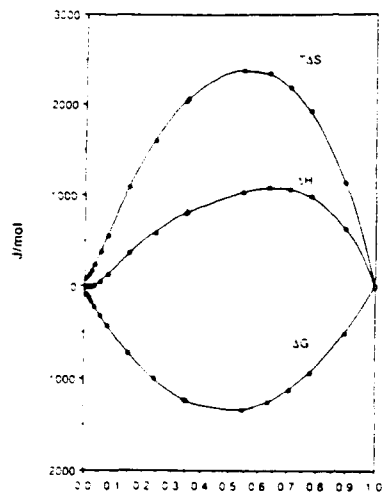


Figure 6. Shift, in cm^{-1} , from 2249 cm^{-1} for 1.9 M CH_3CN in a variety of protic solvents. The error bars are $\pm \sigma$ from a minimum of three replicate measurements. The linear equation is $y = 1.5 + 0.069x$. R = 0.97. All dielectric constant values were taken from ref 39.

UNIT NO. 1010
Gal. 13 AC5B11 AC000762K V-63 1010

60319



CAP00 : Figure 7 Excess thermodynamic properties of the CH₃CN/water
CAP06 : mixture. ΔH^E from ref 43 and ΔG^E from ref 31.

The number of words in this manuscript is 1308.

The manuscript type is A

Author Index Entries

Rowlen, K. L.

Harris, J. M.

Text Page Size Estimate = 4.5 Pages

Graphic Page Size Estimate = 1.0 Pages

Total Page Size Estimate = 5.8 Pages

14

Acetanilid

